The structure and large magnetocaloric effect in rapidly quenched $LaFe_{11.4}Si_{1.6}$ compound

2004 J. Phys.: Condens. Matter 16 8043

(http://iopscience.iop.org/0953-8984/16/45/026)

INSTITUTE OF PHYSICS PUBLISHING JOURNAL OF PHYSICS: CONDENSED MATTER

J. Phys.: Condens. Matter **16** (2004) 8043–8051 PII: S0953-8984(04)85303-7

The structure and large magnetocaloric effect in rapidly quenched $LaFe_{11.4}Si_{1.6}$ compound

X B Liu[1], Z Altounian[1,3] and G H Tu[2]

[1] Center for the Physics of Materials, Department of Physics, McGill University, 3600 University Street, Montreal, QC, H3A 2T8, Canada
[2] Physics Department, Nanjing Normal University, Nanjing, Jiangsu, People's Republic of China

E-mail: zaven@physics.mcgill.ca

Received 24 August 2004
Published 29 October 2004
Online at stacks.iop.org/JPhysCM/16/8043
doi:10.1088/0953-8984/16/45/026

Abstract

The structure and magnetocaloric effect (MCE) of rapidly quenched $LaFe_{11.4}Si_{1.6}$ compound were investigated by means of x-ray diffraction analyses and magnetic measurements. The rapid quenching greatly facilitates the formation of the cubic $La(Fe, Si)_{13}$ (1:13 structure) in $LaFe_{11.4}Si_{1.6}$ alloy. Rietveld analyses indicate that about 22 wt% of the 1:13 phase is formed in rapidly quenched $LaFe_{11.4}Si_{1.6}$ alloy. A subsequent very brief annealing (1273 K/20 min) of the as-quenched alloy is sufficient for the formation of a single-phase 1:13 structure. Magnetic behaviour near T_C indicates the occurrence of a field induced magnetic transition above T_C, which is responsible for the large magnetic entropy change ΔS in annealed rapidly quenched $LaFe_{11.4}Si_{1.6}$ alloy. Comparing with annealed arc melted alloy, the annealed rapidly quenched alloy shows a smaller ΔS at or slightly below T_C, where the magnetocaloric effect mainly originates from the temperature induced magnetic transition. On the other hand, the peaks of ΔS above T_C for the two alloys are almost identical, which is mainly due to the field induced magnetic transition. The results indicate that ΔS due to a temperature induced magnetic transition is sensitive to the microstructure while the MCE related to a field induced magnetic transition is not.

1. Introduction

Research interest in the giant magnetocaloric effect (MCE) at room temperature has been considerably enhanced since the discovery of the giant MCE materials $Gd_5Si_2Ge_2$ (magnetic entropy change $\Delta S = 18.5\ \mathrm{J\ kg^{-1}\ K^{-1}}$ under a 5 T field at $T_C = 276$ K), whose MCE exceeds the reversible MCE based on a second-order magnetic transition in any known magnetic

[3] Author to whom any correspondence should be addressed.

material by at least a factor of 2 [1]. The most important feature is that it undergoes a simultaneous first-order structural and magnetic transition induced by temperature or/and external magnetic field, which is responsible for the large magnetic entropy change near T_C. Large magnetic entropy changes due to a first-order magnetic transition near T_C are also observed in other systems such as $(La_{1-x}Ca_x)MnO_3$, $MnFeP_{1-x}As_x$ and $La(Fe, Si)_{13}$ [2–4].

$LaFe_{13-x}Si_x$ pseudobinary compounds with the $NaZn_{13}$ structure ($1.5 \leqslant x \leqslant 2.5$) were first reported by Palstra *et al* [5] twenty years ago and are enjoying renewed interest [6–8] in the magnetic materials community due to the observation of a large MCE in $LaFe_{11.4}Si_{1.6}$ compound, which shows a large magnetic entropy change, $\Delta S = 19.4\ J\,kg^{-1}\,K^{-1}$ at $T_C = 208$ K [4]. The large magnetocaloric effect is due to the strong first-order magnetic transition at T_C and the field induced metamagnetic transition above T_C. A large negative lattice expansion is observed around T_C by means of powder x-ray diffraction and neutron diffraction [7, 9]. With increasing Si content, the maximum magnetic entropy change decreases rapidly and the order of magnetic transition changes from first order to second order [8]. Compounds $La(Fe_{1-x}Co_x)_{11.4}Si_{1.6}$ with $x = 0$–0.1 display T_C from about 200 to 330 K and their ΔS slowly decreases with increasing Co content [10]. $La(Fe_{1-x}Co_x)_{11.4}Si_{1.6}$ based materials could be good candidates for room temperature magnetic refrigeration application.

However, pseudobinary compounds $La(Fe, Co)_{11.4}Si_{1.6}$ with $NaZn_{13}$ structure are difficult to form. In all reported works on $La(Fe, Co, Si)_{13}$ [4–12], the samples were prepared by induction melting or arc melting, followed by a lengthy (several weeks to two months) annealing at about 1273 K and, in particular, no elaborate study of the phase formation was made for the large MCE alloy with lower Si content. In this work, we successfully prepared $LaFe_{11.4}Si_{1.6}$ compounds with an almost single-phase $NaZn_{13}$ structure using a rapid solidification technique followed by a very brief annealing and report on its structure and magnetocaloric effect.

2. Experimental techniques

$LaFe_{11.4}Si_{1.6}$ alloy was prepared in purified Ar atmosphere by a tri-arc melting method in a Ti-gettered Ar atmosphere. The ingots were remelted several times to achieve compositional homogeneity. The rapidly quenched ribbons with a thickness of 20 μm were prepared by melt spinning using a copper wheel with a wheel surface speed of 50 m s^{-1} in a 50 kPa He atmosphere. The rapidly quenched ribbons and the ingots were sealed in an evacuated quartz tube and annealed at 1273 K for 20 min and two weeks, respectively. The powder x-ray diffraction (XRD) analysis was performed in a Siemens D5000 X-ray Powder Diffractometer with Cu Kα radiation. The quantitative phase analyses are performed by the Rietveld method using the GSAS code [13]. Differential thermal analysis (DTA) was performed in a Perkin-Elmer DTA-7 Analyzer in an Ar gas flow with a heating rate of 40 K min^{-1}. Curie temperatures, T_C^{χ}, were determined from the ac susceptibility (χ_{ac}), using a Quantum Design Physical Property Measurement System (PPMS) magnetometer. The magnetometer was also used for dc magnetization measurements in fields of up to 9 T.

3. Results and discussion

3.1. Phase constituents and crystal structure

Experimental and Rietveld fitted x-ray diffraction patterns for arc melted $LaFe_{11.4}Si_{1.6}$ alloy are displayed in figure 1. The identified phases are α-(Fe, Si), tetragonal LaFeSi with $a = 4.108$ Å and $c = 7.170$ Å and about 6 wt% of cubic $La(Fe, Si)_{13}$ compound (1:13).

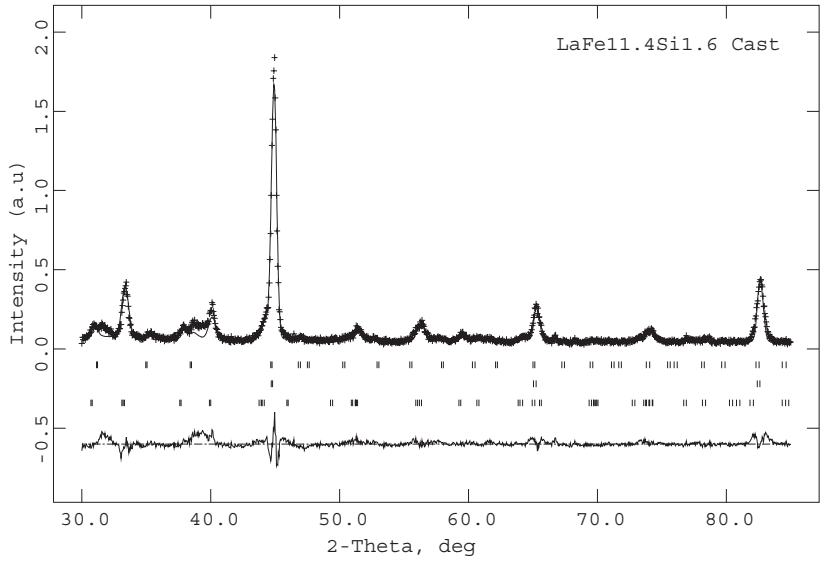

Figure 1. Experimental (crosses) and Rietveld fitted (solid curve) x-ray diffraction patterns for arc melted $LaFe_{11.4}Si_{1.6}$ alloy. The Bragg position marks are for LaFeSi, α-(Fe, Si) and La(Fe, Si)$_{13}$ phases from bottom to top.

Table 1. Phase constituents for $LaFe_{11.4}Si_{1.6}$ compounds.

	α-(Fe, Si) (wt%)[a] fitted/calculated	LaFeSi (wt%) fitted/calculated	La(Fe, Si)$_{13}$ (wt%) fitted/calculated
Arc melted (AM)	68/68	26/25	6/7
AM + annealing	5/3.6	0/1.4	95/95
Rapidly quenched (RQ)	59/59	19/22	22/19
RQ + annealing	4/3	0/1	96/96

[a] Assuming the alloy has the exact nominal composition and the fitted value of the phase with the largest quantity is accurate.

The fitted lattice constant of α-(Fe, Si) is 2.856 Å, slightly smaller than that of α-Fe (2.866 Å), indicating that some of the Si was dissolved in α-Fe. As shown in table 1, the Rietveld derived quantity of each phase is almost the same, within error, as the calculated value assuming that the alloy has the exact nominal composition and the fitted value of the phase with the largest quantity (α-(Fe, Si)) is accurate.

As shown in figure 2, x-ray diffraction data indicate that about 22 wt% of 1:13 phase is formed in the rapidly quenched $LaFe_{11.4}Si_{1.6}$ alloy in addition to α-(Fe, Si) and tetragonal LaFeSi phase. The results indicate that the rapid quenching helps the formation of the 1:13 phase. This can be understood from the solidification process of the $LaFe_{11.4}Si_{1.6}$ alloy. The 1:13 phase is formed by the peritectic transition from α-(Fe, Si) and La-rich liquid phase. The resulting phases are α-(Fe, Si), LaFeSi and a little of the 1:13 phase in the arc melted alloy due to non-equilibrium solidification behaviour. In comparison with the arc melting process case, the $LaFe_{11.4}Si_{1.6}$ liquid alloy is rapidly cooled to the 1:13 single-phase region through the two-phase region of α-(Fe, Si) and La-rich liquid phase during the melt spinning process. The rapid quenching inhibits the precipitation of α-(Fe, Si) in the melting alloy and enhances the formation of the 1:13 phase.

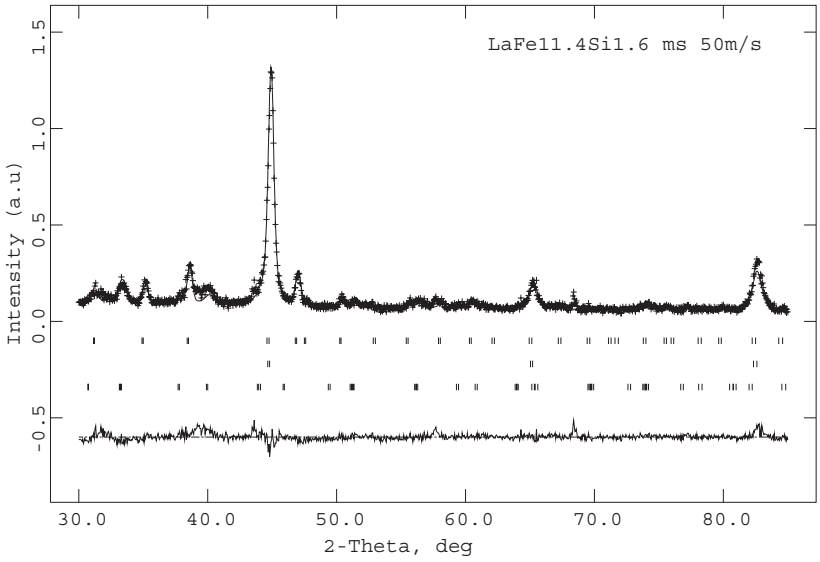

Figure 2. Experimental (crosses) and Rietveld fitted (solid curve) x-ray diffraction patterns for rapidly quenched $LaFe_{11.4}Si_{1.6}$ alloy (50 m s^{-1}). The Bragg position marks are for LaFeSi, α-(Fe, Si) and La(Fe, $Si)_{13}$ phases from bottom to top.

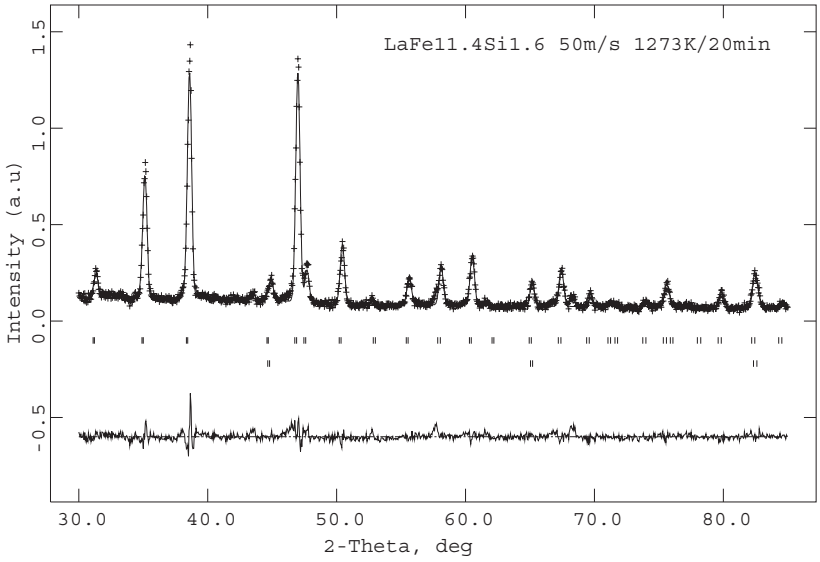

Figure 3. Experimental (crosses) and Rietveld fitted (solid curve) x-ray diffraction patterns for rapidly quenched $LaFe_{11.4}Si_{1.6}$ alloy after an annealing treatment (1273 K/20 min). The Bragg position marks are for α-(Fe, Si) and La(Fe, $Si)_{13}$ phase from bottom to top.

In addition, there is one small peak around 68.5° for the as-quenched sample, which is also observed in the sample after annealing (figure 3). The peak is most likely due to some La–Si phase. The quantitative phase analysis results are also listed in table 1, which again yields the same values, within error, as the calculated ones.

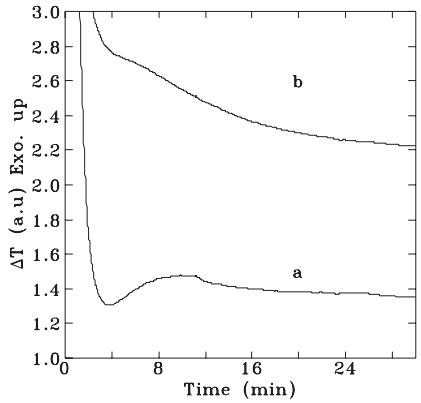

Figure 4. Isothermal DTA curves at 1223 K for (a) rapidly quenched and (b) arc melted $LaFe_{11.4}Si_{1.6}$ alloys.

A nearly single phase with 1:13 structure (96 wt%) is formed after annealing at 1273 K for 20 min for the rapidly quenched sample (figure 3). The fitted lattice constant, a, is 11.476 Å. A small amount (4 wt%) of α-(Fe, Si) is still present. As mentioned above, it often takes several weeks to attain an almost single-phase 1:13 sample by annealing the arc melted samples. These differences could be ascribed to the difference in microstructure between arc melted and rapidly quenched alloys. The rapid quenching results in fine crystal grain microstructure and the presence of a relatively large amount of 1:13 phase, which will accelerate the formation of the 1:13 structure during the subsequent annealing process due to the reduced diffusion distance and greater number of nuclei of the 1:13 phase. A complete analysis of a microstructural study using transmission electron microscopy (TEM) is in preparation.

In order to gain more insight into the formation of 1:13 structure, differential thermal analysis (DTA) is performed. During the isochronal heating, the only thermal peak detected is the melting point of 1330 K for rapidly quenched $LaFe_{11.4}Si_{1.6}$ alloy between 373 and 1673 K. This is due to the relatively small thermal effect for the formation of the 1:13 phase, as the heat of mixing for $LaFe_{11.4}Si_{1.6}$ alloy is small. According to the Meidema model [14], the heat of mixing between La and Fe is positive, while that between La and Si, or between Fe and Si is negative. This explains why the binary La–Fe compound does not exist, while a small amount of Si can stabilize the 1:13 structure in $LaFe_{11.4}Si_{1.6}$ alloy. This is also one reason that the 1:13 structure is difficult to form in $LaFe_{13-x}Si_x$ alloy with low Si content. Figure 4 displays an isothermal DTA curve for the rapidly quenched $LaFe_{11.4}Si_{1.6}$ alloy at 1223 K. An exothermal peak is clearly seen at about 10 min for the rapidly quenched sample, indicating the formation of a substantial amount of 1:13 phase during the heating process. The isothermal DTA results conform to the fact that the formation of 1:13 in rapidly quenched alloy needs a very short annealing time (1273 K/20 min) while that in arc melted alloy needs two weeks of annealing at the same temperature.

3.2. Magnetic behaviour near T_C

Figure 5 displays the thermomagnetic curve, M–T, measured under a dc magnetic field of 0.01 T, for the annealed rapidly quenched (ARQ) $LaFe_{11.4}Si_{1.6}$ compounds. The magnetization changes very sharply at $T_C = 202$ K, implying a large magnetic entropy change. The M–T curve also indicates the presence of a very small amount of ferromagnetic phase with a much higher T_C besides the main phase 1:13. This minor ferromagnetic phase is α-(Fe, Si), as indicated by x-ray diffraction results (figure 3).

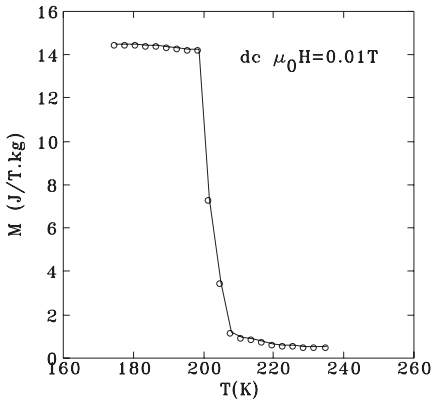

Figure 5. The thermomagnetic curve M–T for rapidly quenched $LaFe_{11.4}Si_{1.6}$ compound after an annealing treatment (1273 K/20 min).

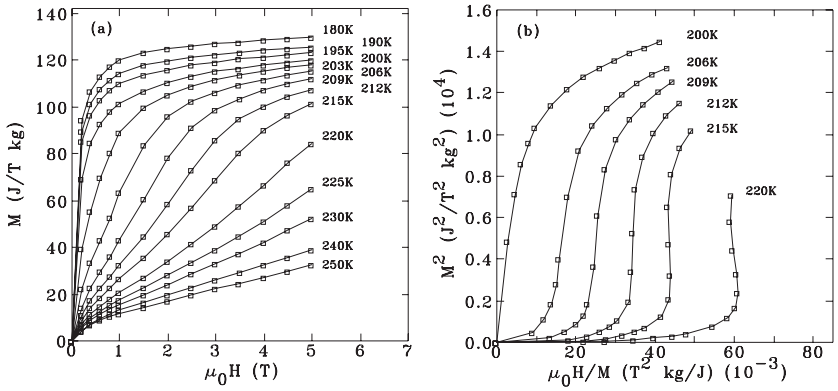

Figure 6. (a) The magnetization, $M(\mu_0 H)$, of $LaFe_{11.4}Si_{1.6}$ at different temperatures. (b) Arrott plots for $LaFe_{11.4}Si_{1.6}$ near T_C.

Figure 6(a) displays the magnetization curves, $M(T, H)$, of the ARQ $LaFe_{11.4}Si_{1.6}$ alloy at different temperatures near T_C. The corresponding Arrott plots are shown in figure 6(b). The rapid increase in M near about 2–3 T in the M–H curves and the inflection point and negative slope in Arrott plots above T_C indicate the occurrence of a first-order field induced itinerant-electron metamagnetic transition from the paramagnetic to the ferromagnetic state above T_C, which is similar to that of annealed arc melted (AAM) $LaFe_{11.4}Si_{1.6}$ compound [7, 8].

The magnetic behaviour near T_C can be further understood from the derivative of the magnetization, $\frac{dM}{dH}$, versus the applied magnetic field at different temperatures. As shown in figure 7, $\frac{dM}{dH}$ decreases very rapidly from a large value at low external field and then levels off to a very small value with increasing applied field below T_C (e.g. 200 K), which is a typical feature of the magnetization behaviour of a soft ferromagnet. A peak in the $\frac{dM}{dH}$–H curve above T_C (e.g. 209 K) is clearly seen in figure 7. This implies that the magnetization increases rapidly when the applied field approaches a critical value corresponding to the peak. This is the signature of a field induced magnetic transition from the paramagnetic to the ferromagnetic state above T_C. Upon further increase in H, the value of $\frac{dM}{dH}$ approaches a constant, consistent with a typical paramagnetic behaviour. For temperatures somewhat higher than T_C, such as

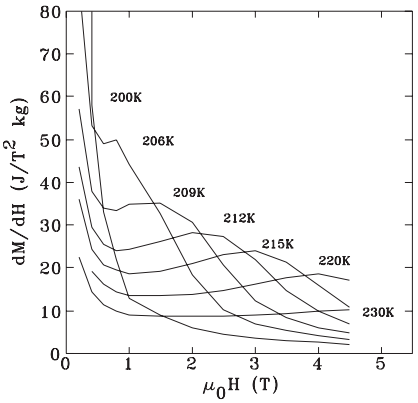

Figure 7. Derivative curves of magnetization via applied magnetic field $\frac{dM}{dH}$–H for annealed rapidly quenched $LaFe_{11.4}Si_{1.6}$ alloy.

230 K, no field induced magnetic transition is observed under an applied field of 5 T. The critical field for the occurrence of a field induced magnetic transition is about 1–3 T between 200 and 215 K.

3.3. The magnetocaloric effect

The MCE was approximately evaluated from the isothermal magnetic entropy change using magnetic measurements. The magnetic entropy change ΔS is calculated via Maxwell's thermodynamic relation:

$$\Delta S(T, H) = \int_0^H \left(\frac{dM}{dT}\right) dH. \tag{1}$$

The accuracy of the ΔS calculated using this technique is about 3–10% [15].

As shown in figure 6(a), a nonlinear initial increase in magnetization is clearly seen in the M–H curve for temperatures much higher than T_C (e.g. 250 K) due to the presence of a small amount of α-(Fe, Si) in the sample, which conforms to the XRD (figure 3) and M–T results (figure 5). The contribution of α-(Fe, Si) to the magnetic entropy change is neglected due to its high T_C.

Figure 8 shows the temperature dependence of the magnetic entropy change of the ARQ (a) and the AAM (b) $LaFe_{11.4}Si_{1.6}$ compounds under different external fields. For both samples, the broadening of the ΔS peak above T_C is obviously larger than that below T_C and the ΔS peak position shifts to a higher temperature with increasing applied field because of the occurrence of a field induced magnetic transition. The ΔS peak position is at about 201 K for 1 T while the peak is at about 207 K for 5 T. The maximum magnetic entropy change, ΔS, is almost the same, within the error, and 20.3 J kg^{-1} K under a magnetic field change of 5 T for both samples. However, ΔS, under lower magnetic fields (e.g. 1 T, figure 8), for the ARQ sample is much smaller than that of the AAM one. Further, the ΔS peaks of the ARQ alloy are slightly broader.

Figure 9 displays the applied field dependence of ΔS at 201 and 207 K for ARQ and AAM alloys. For both samples, the shapes of ΔS–H curves at and above T_C are very different, indicating the different origins of the magnetic entropy change. The magnetic entropy change ΔS at or slightly below T_C mainly originates from the temperature induced magnetic transition and, therefore, ΔS increases rapidly with the magnetic field at low fields and then increases

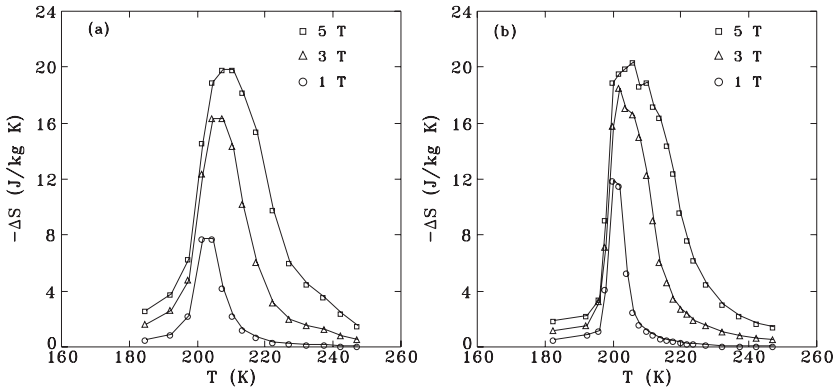

Figure 8. The temperature dependence of the magnetic entropy change for $LaFe_{11.4}Si_{1.6}$ under different magnetic fields: (a) rapidly quenched (50 m s^{-1}) and annealed (1273 K/20 min); (b) arc melted and annealed (1273 K/2 weeks).

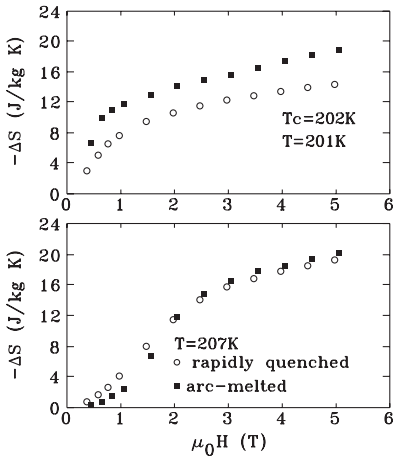

Figure 9. The applied field dependence of ΔS at 201 and 207 K for $LaFe_{11.4}Si_{1.6}$ alloys. The initial applied field is zero.

almost linearly with the field. For temperatures above T_C, ΔS increases rapidly as the magnetic field approaches a critical value and the variation of ΔS takes an S-shape form, due to the field induced magnetic transition above T_C.

It is interesting to note that the magnetic entropy change ΔS for the ARQ sample is smaller than that of the AAM sample at T_C (201 K). As noted above (figure 7), the ΔS peaks are also slightly broader. This can be understood from the sum rule [16] derived from equation (1):

$$\int_0^\infty \Delta S(T, H)\,\mathrm{d}T = -HM_0. \tag{2}$$

This rule implies that for materials with the same saturation magnetization, M_s, those (such as the AAM sample) with a high magnetic entropy change at a given temperature will have low ΔS at other temperatures. It is reasonable that the ARQ sample displays a lower peak value under low external fields (e.g., 1 T), but has a broader peak. A similar situation is also observed for a melt spun $DyCo_2$ compound [17]. We believe that this could be attributed to the fine crystalline grains and the exchange interaction between them in the rapidly quenched

sample. However, the magnetic entropy changes ΔS for the two kinds of alloys (ARQ and AAM) are almost the same, within error, above T_C (207 K). ΔS for the ARQ alloy seems slightly larger than that of the AAM compound as the applied field is less than the critical field for the occurrence of the field induced magnetic transition, while ΔS for the ARQ is slightly smaller than that for the AAM alloy above the critical field. The results indicate that the microstructure has little effect on the field induced magnetic phase transition in $LaFe_{11.4}Si_{1.6}$ alloys.

4. Conclusion

Rapid quenching helps the formation of the cubic 1:13 structure in $LaFe_{11.4}Si_{1.6}$ alloys. Rietveld fitting indicates that about 22 wt% of 1:13 phase is formed in rapidly quenched $LaFe_{11.4}Si_{1.6}$ alloy while about 6 wt% of 1:13 structural phase is formed in the arc melted ingot. A nearly single-phase 1:13 structure is formed in rapidly quenched $LaFe_{11.4}Si_{1.6}$ alloy after a brief annealing (1273 K/20 min) while the arc melted sample needs at least two weeks of annealing to form the same phase at the same temperature, a three-orders-of-magnitude reduction in annealing time. Rapid quenching is an effective preparation method for the magnetocaloric cubic $LaFe_{11.4}Si_{1.6}$ based compounds, which is quite useful from an industrial processing point of view.

Similar to the case for AAM $LaFe_{11.4}Si_{1.6}$ compound, magnetic behaviour indicates the occurrence of a field induced magnetic transition above T_C, which is responsible for the large magnetic entropy change in ARQ alloy. Compared to AAM alloys, the ARQ alloy shows a smaller ΔS at or slightly below T_C. The values of ΔS above T_C, where the field induced magnetic transition occurs, are almost the same for both alloys. We conclude that ΔS at or slightly below T_C is mainly due to the temperature induced magnetic transition, while the ΔS peak above T_C originates from the field induced magnetic transition. The results indicate that ΔS due to the temperature induced magnetic transition is sensitive to the microstructure while that involving a field induced magnetic transition is not.

References

[1] Pecharsky V K and Gschneidner K A 1997 *Appl. Phys. Lett.* **70** 3299
[2] Morelli D T, Mance A M, Mantese J V and Micheli A L 1996 *J. Appl. Phys.* **79** 373
[3] Tegus O, Bruck E, Buschow K J H and de Boer F R 2002 *Nature* **415** 150
[4] Hu F X, Shen B G, Sun J R, Cheng Z H, Rao G H and Zhang X X 2001 *Appl. Phys. Lett.* **78** 3675
[5] Palstra T T M, Mydosh J A, Nieuwenhuys G J, van der Kraan A M and Buschow K H J 1983 *J. Magn. Magn. Mater.* **36** 290
[6] Zhang X X, Wen G H and Wang F W 2000 *Appl. Phys. Lett.* **77** 3072
[7] Fujita A, Fujieda S and Fukamichi K 2002 *Appl. Phys. Lett.* **81** 1276
[8] Liu X B, Altounian Z and Ryan D H 2003 *J. Phys.: Condens. Matter* **15** 7385
[9] Wang F W, Wang G, Hu F, Kurbakov A, Shen B and Cheng Z 2003 *J. Phys.: Condens. Matter* **15** 5269
[10] Liu X B and Altounian Z 2003 *J. Magn. Magn. Mater.* **264** 209
[11] Tang W H, Liang J K, Chen X L and Rao R H 1994 *J. Appl. Phys.* **76** 4095
[12] Rao R H, Liang J K, Zhang Y L, Tang W H and Cheng X R 1996 *J. Appl. Phys.* **80** 336
[13] Larson A C and Von Dreele R B 1994 General structure analysis system (GSAS) *Los Alamos National Lab. Report* LAUR 86-748
[14] Miedema A R, Boom F R and de Boer F R 1992 *Physica* B **182** 1
[15] Pecharsky V K and Gschneidner K A Jr 1999 *J. Magn. Magn. Mater.* **200** 44
[16] McMichael R D, Shull R D, Swartzendruber L J, Bennett L H and Watson R E 1992 *J. Magn. Magn. Mater.* **111** 29
[17] Wang D H, Tang S L, Liu H D, Li S D, Zhang J R and Du Y W 2001 *Japan. J. Appl. Phys.* 1 **6815** 2001